

NMR Study on Solubilization of Sterols and Aromatic Compounds in Sodium Taurodeoxycholate Micelles

Keisuke Matsuoka,*[1] Shigeaki Ishii,[1] Chikako Honda,[1] Kazutoyo Endo,[1] Akio Saito,[2] Yoshikiyo Moroi,[3] and Osamu Shibata[3]

[1]Department of Physical Chemistry, Showa Pharmaceutical University, 3-3165 Higashi-Tamagawagakuen, Machida, Tokyo 194-8543

[2]Organic Reaction Chemistry, Showa Pharmaceutical University, 3-3165 Higashi-Tamagawagakuen, Machida, Tokyo 194-8543

[3]Department of Biophysical Chemistry, Faculty of Pharmaceutical Sciences, Nagasaki International University, 2825-7 Huis Ten Bosch, Sasebo 859-3298

Received June 21, 2007; E-mail: matsuoka@ac.shoyaku.ac.jp

The solubility of cholesterol in the binary solubilizates system (cholesterol and β-sitosterol) of a sodium taurodeoxycholate solution decreased to almost half of that in the single cholesterol system. On the other hand, the cholesterol solubilities in other binary other systems (cholesterol and certain aromatics) of those solutions were the same as that of the single cholesterol system. The results of competitive solubilization between sterols and aromatics suggested that both were solubilized at different solubilization sites of a micelle. Their molecular dynamics and solubilization sites were measured by the ^{1}H NMR method. The rotating-frame nuclear Overhauser effect and exchange spectroscopy (ROESY) contour plot of aromatics solubilized micellar solution exhibited direct cross-peaks between the aromatics and bile salt of 19-methyl protons. The observed ROESY spectra of the sterol-solubilized solutions were almost identical to those of the pure micellar solution. The spin-lattice relaxation time (T_1) for aromatics solubilized in the micellar solutions increased for 18-, 19-, and 21-methyl protons of the bile salt in comparison with those of a pure micellar solution, which indicated that the micellar core changed to a loosely packed state owing to the penetration of aromatics. On the other hand, the T_1 values for sterols solubilized in micelles were lesser than those for pure micellar solutions for almost all proton positions, which suggested that the sterols were compatible with the micelle. These results indicated that the aromatics were solubilized in micellar palisade layer interacting with bile salt of methyl protons, whereas, the sterols were solubilized to match the micellar structure via the steroids interaction.

High concentration of absorbed cholesterol in blood is one of the causes of cardiovascular diseases, which is currently a grave medical concern due to the recent changes in dietary styles.[1–3] Plant sterols have been taken preventive measures against high cholesterol level and investigated as a hypocholesterolemic agent.[4,5]

During a competitive solubilization study (of cholesterol and other compounds), the authors found that the cholesterol solubility for a binary mixed solubilizate system (cholesterol and β-sitosterol) was almost half of that in a pure cholesterol system. On the contrary, the mutual solubilities of cholesterol and pyrene were not inhibited in the binary mixed system. The above-mentioned competitive solubilization between cholesterol and other compounds may have originated from the solubilization site in bile salt micelles. Recently, powerful methods of NMR have the advantage of detecting intramolecular and intermolecular interactions; moreover, their dynamics can be directly estimated by the interactive atoms in a micellar solution. The micelle formation of bile salts,[6–8] solubilization,[9,10] and the interactions of bile salts and proteins[11] have been studied by the ^{1}H NMR experiments. Two-dimensional NMR was directly used to determine the micellar structure and solubilization site in a micelle.[9] Moreover, the study of the spin-lattice relaxation time (longitudinal relaxation time: T_1) revealed a micellar structure based on the molecular dynamics of the rotational motion.[7,12]

The aim of the present study is to find the solubilization site in sodium taurodeoxycholate micelles by the NMR method when sterols or aromatic compounds are solubilized into the micelles. The competitive solubilization between cholesterol and sterol is inferred to be closely linked to the cholesterol-lowering mechanism during the ingestion of sterols.

Experimental

Materials. Sodium taurodeoxycholate (NaTDC) was of guaranteed reagent grade (ca. 97%, Sigma). Organic impurities were removed first by first washing with diethyl ether, following which the salts were recrystallized from ethanol. Their purities were checked by thin-layer chromatography, which showed a single spot in their chromatograph. Their chemical structures are shown in Fig. 1.

Cholesterol of guaranteed reagent grade (Sigma) was recrystallized from ethanol, and the purity was checked by elemental analysis: C, 83.79 (83.87)% and H, 11.97 (11.99)%, where the values in parentheses are the calculated ones. β-Sitosterol was purchased from Tama Biological, Japan, and its high purity was confirmed

Published on the web December 13, 2007; doi:10.1246/bcsj.80.2334

by gas chromatography. The molecular structures of sterols are shown in Fig. 1.

Naphthalene and pyrene of guaranteed reagent grade (Wako Pure Chemical, Japan) were purified by repeated recrystallizations from the ethanol solution.

Deuterium oxide (D, 99%, CIL), chloroform-D + 0.05% TMS (D, 99.8%, CIL), and 3-(trimethylsilyl)propionic acid-D4 sodium salt (98%, MERCK) were used as solvents and as an internal standard in the ^{1}H NMR spectrum, respectively.

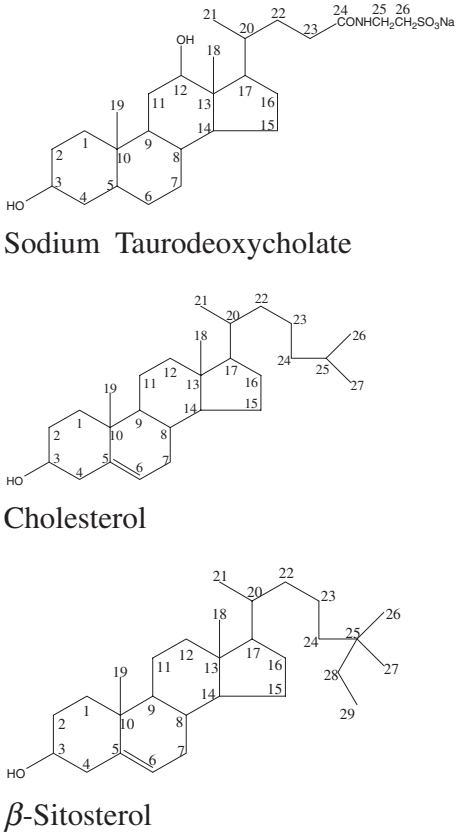

Fig. 1. Molecular structure of the bile salts and sterols and numbering of the carbon atoms.

Solubilization. Three mL of the 15 mM (1 M = 1 mol dm^{-3}) NaTDC solutions (solvent: D_2O) and a certain amount of solid solubilizates that was sufficient to produce a saturated solution were taken in a 10-mL injector tube.[13] The solutions were stirred for 24–72 h until the system achieved equilibrium. Equilibrium was attained within 24 h in most cases depending on the time-dependence of the solubilized amount. The separation of coexisting solids was performed by filtration through a membrane filter with a pore size of 0.2 μm (Millipore Co. FGLP01300) by applying pressure on the injector in a thermostat controlled at 308.2 ± 0.1 K. The concentration of each sterol in the filtrates was determined using a spectrophotometer (Hitachi U-4100) and an enzyme assay determiner TC555 (Kyowa Medex, Japan).[14,15] With regard to aromatics, the maximum solubility was determined from the absorbance of the filtrates using each molar extinction coefficient.[16] In the case of a binary solubilizates system (cholesterol and β-sitosterol crystal), the concentration of each sterol was measured by ^{3}H–^{14}C radioactivity. The details of the operation are described in our previous report.[13]

NMR Measurements. NMR samples were prepared by adding 30 μL of internal standard deuterium oxide solution (TSP and corresponding concentration of NaTDC) to a 670-μL filtrate solution. NMR experiments were performed at 308.2 ± 0.5 K using a JEOL AL-300 spectrometer for determining T_1 and a JEOL Alpha 500 spectrometer for determining the ROESY spectrum.

The T_1 values were obtained using the 180°–τ–90° standard inversion recovery technique. The peak intensities at ten different interpulse delays were determined. The measurement condition, 90° pulse of 12.1 μs, 180° pulse of 24.2 μs, relaxation delay of 6 s, and four times dummy scans was employed in predominant and calibration experiments.

ROESY for all solutions was measured at a mixing time of 300 ms using standard three-pulse sequences, where the mixing time was selected on the basis of previous experiments with varying mixing times. Their mixing time for solubilized solutions were confirmed by auto tuning system with apparatus, which kept within the range of 282–322 ms. This agreed well with other literature values for similar systems.[9] The obtained data were processed using JEOL software ALLICE II (fully automatic processing system).

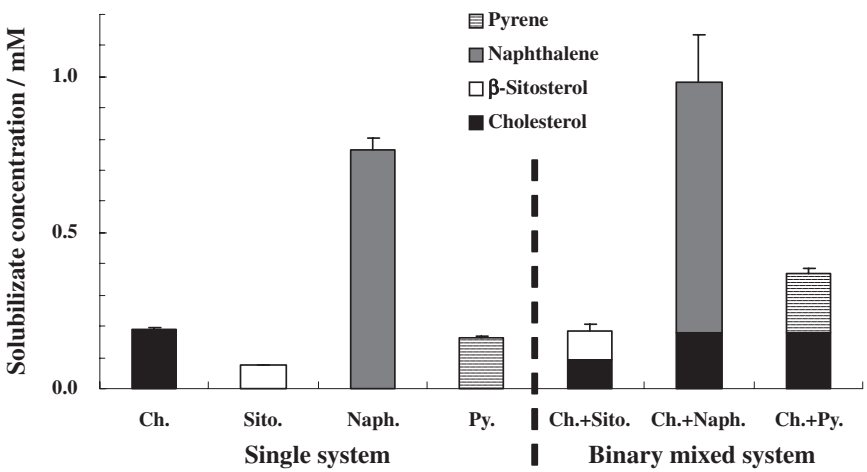

Fig. 2. Solubility change of cholesterol, β-sitosterol, and aromatic compounds in a single solubilizate system (left-hand side) and solubilizate of cholesterol and other compounds in a binary mixed system (right-hand side) in a 15 mM NaTDC solution.

Results and Discussion

Competitive Solubilization of Cholesterol and Solubilizates. The molecular structure of NaTDC is shown in Fig. 1. The characteristic properties of NaTDC micelles include lower critical micelle concentration (3–5 mM), relatively large aggregation number of micelles (15.9), and higher solubility for cholesterols other than bile salt micelles.[17] The high solubilization capacity is advantageous for measuring the NMR spectrum, which is required for accurately determining the greater than sub-mM concentrations in this experiment. This research originated from our previous experimental result, which showed that the solubility of cholesterol in a bile salt solution depended on the presence of other competitive solubilizates.[13] The maximum solubilities of single and binary mixed solubilizates in a 15 mM NaTDC solution (D_2O) are shown in Fig. 2. The left-hand side of Fig. 2 shows that β-sitosterol and pyrene possess similar solubilities in a single cholesterol system. However, they had different effects on the lowering of cholesterol solubility in a binary mixed system, as shown in the right-hand side of Fig. 2. β-Sitosterol could lower the cholesterol solubility in a binary mixed system, while pyrene had no influence. This difference may result from the intrinsic variances in their molecular structures. Both cholesterol and β-sitosterol may compete and occupy the same solubilization site in bile salt micelles since their molecular structures are almost identical. On the other hand, pyrene has a planar molecular structure; therefore, it may not compete with cholesterol for the solubilization site. In the binary system of naphthalene and cholesterol, the cholesterol solubility was not hindered by aromatic compound of naphthalene in a similar description as pyrene. The location where the solubilizates are solubilized in the bile salt micelle must be determined; this may clarify the mechanism of decreased cholesterol solubility and the cause of competitive solubilization.

^{1}H NMR Spectrum. Figure 3a shows the ^{1}H NMR spectrum of the 15 mM NaTDC solution at 308.2 K. Each ^{1}H chemical shift can be attributed to the respective proton position on the basis of several previous reports.[18–21] Considering the complicated form of the spectra, only sharp and characteristic spectra are selected. The spectra of each maximum solubilized cholesterol (Fig. 3b), β-sitosterol (Fig. 3c), naphthalene (Fig. 3d), and pyrene (Fig. 3e) in 15 mM NaTDC solutions are shown in Figs. 3b–3e, respectively. Each saturated concentration in a 15 mM NaTDC solution corresponds to the left-hand side of Fig. 2. Moreover, the ^{1}H NMR spectra of cholesterol (7.8 mM) and β-sitosterol (3.5 mM) in a $CDCl_3$ solution are given in Figs. 3f and 3g, respectively. Good NMR experiments can be performed by distinguishing between the proton spectra from a solubilizate and NaTDC when adding a solubilizate to NaTDC micellar solutions. A comparison between Fig. 3a (NaTDC) and Fig. 3f (cholesterol solubilizate) shows that their spectra are almost overlapped for steroid rings and thus each part of the spectrum cannot be distinguished. However, the total interactions between micelles and sterols in saturated micellar solutions appear to have relatively strong intensities at ca. 1.3 and 3.7 ppm in Figs. 3b and 3c, which results from the contribution of each steroid ring (NaTDC and sterols). With regard to the proton spectra between aromatics

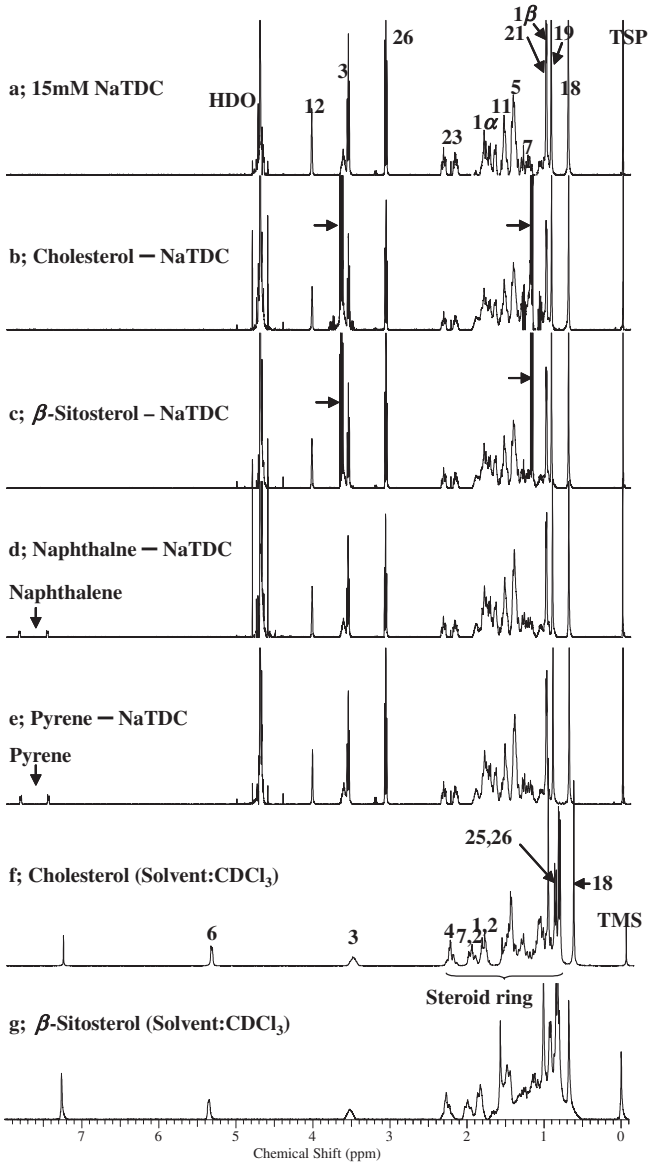

Fig. 3. The comparative ^{1}H NMR spectra of the solubilization systems at 308.2 K. The figure shows the following spectra. a: pure system of 15 mM NaTDC (solvent: D_2O); b: saturated cholesterol–NaTDC; c: saturated β-sitosterol–NaTDC; d: saturated naphthalene–NaTDC; e: saturated pyrene–NaTDC; f: pure system of 7.8 mM cholesterol (solvent: $CDCl_3$); and g: pure system of 3.5 mM β-sitosterol (solvent: $CDCl_3$). The saturated concentrations of the solubilizates correspond with those shown in Fig. 2. The arrows in Figs. 3b and 3c indicate one of the proton spectra most affected by solubilization in comparison with the pure system shown in Fig. 3a.

and NaTDC, the spectra of solubilized naphthalene and pyrene were clearly observed downfield, as shown in Figs. 3d and 3e. The spectra of the solubilizates proved that they were sufficiently solubilized in the NaTDC micellar solution, and the 2D ROESY spectrum could be used to measure the direct interaction between the micelle and solubilizates. The chemical shifts of the saturated solubilizate of an NaTDC solution (15 mM) are summarized in Table 1. It is observed that several

Table 1. Chemical Shift of ^{1}H NMR for Saturated Solubilizates of NaTDC Solutions (15 mM) at 308.2 K[a)]

	Chemical shift of satulated solubilizate of NaTDC solution (15 mM)/ppm				
H position	Pure system	Cholesterol	β-Sitosterol	Naphthalene	Pyrene
1α	1.78	1.78	1.78	1.78	1.78
1β	0.99	0.99	0.99	0.99	0.99
3β	3.55	3.55	3.55	3.55	3.55
5β	1.39	1.39	1.39	1.39	1.39
11α	1.54	1.54	1.54	1.53	1.53
12β	4.03	4.03	4.03	4.04	4.04
18	0.71	0.71	0.71	0.70	0.70
19	0.93	0.93	0.93	0.91	0.91
21	1.00	1.00	1.00	1.00	1.00
23β	2.23	2.23	2.23	2.23	2.23
25α	3.57	3.57	3.57	3.57	3.57
26α	3.08	3.08	3.08	3.08	3.08

a) The concentrations of the solubilizates correspond with those shown in Fig. 2.

chemical shifts of the micellar solution including aromatics (naphthalene and pyrene) are different from those of the original pure micellar solution. The chemical shifts of NaTDC with 11α and 12β change from the original solution to 0.01 ppm downfield, whereas those of methyl group with 18 and 19 protons change to 0.01–0.02 ppm upfield. The slight change in chemical shift implies that the proton positions in NaTDC micelles are directly or indirectly influenced by the solubilization of aromatics. These specific protons closely agreed with the key protons estimated by the ROESY and T_1 measurements. On the other hand, the solubilizations of cholesterol and sitosterol into micelles have no effect on their chemical shifts.

ROESY Spectrum. The ROESY spectra of solubilized sterols and aromatics in the 15 mM NaTDC solutions were measured to estimate the key proton for the direct interaction between the micelle and solubilizate. The technique has the advantage of direct investigation of intramicellar and intermicellar interactions by measuring the cross-relaxation.[9] Fortunately, the NMR signal of the aromatics does not overlap with that of NaTDC, as shown in Figs. 3d and 3e, which is observed for the direct assignment of cross-peaks (aromatics-NaTDC). Moreover, the method provides several insights about the micellar model structure. The contour plot of the ROESY spectrum for the NaTDC solution (pure micellar state, 15 mM) is shown in Fig. 4a. The monomer state of the solution (1 mM) was used to understand the intermolecular cross-peak of the monomer state; the cross-peak did not exist except for pairs of vicinal protons of NaTDC molecules (omission). Moreover, the ROESY spectra for the saturated solubilizates of micellar solutions (15 mM NaTDC) are given in Figs. 4b (cholesterol), 4c (β-sitosterol), 4d (naphthalene), and 4e (pyrene). The obtained cross-peaks for the solutions were analyzed by JEOL software ALLICE II (fully automatic processing system). The complicated, inseparable spectra have already been excluded from the data. Therefore, the analysis focused on the separable chemical shift of NaTDC, using the data given in Table 1. The presences of the cross-peaks for the solutions are summarized in Table 2. The signal intensities are not considered in this study. As shown in Table 2, the cross-peaks of 12β–18-methyl, 12β–21-methyl, 18-methyl–19-methyl, 18-methyl–21-methyl, and 19-methyl–21-methyl protons greatly contribute to micelle formation in the pure 15 mM NaTDC solution (Fig. 4a). It appears that methyl groups at the 18, 19, and 21 positions perform the important function of aggregating NaTDC molecules by hydrophobic interactions. Other pairs were also observed for the NaTDC solution, according to another report.[6] The cross-peak patterns of cholesterol and β-sitosterol-solubilized micelles are almost identical to those for the pure micellar solution, as shown in Figs. 4b and 4c. These results are summarized in Table 2, which also shows that sterols can be solubilized to fit into the micellar structure. A thermodynamic analysis reveals the ΔG° values for solubilization in the NaTDC solution to be -41.7, -47.1, -31.8, and $-19.9\,\mathrm{kJ\,mol^{-1}}$ for cholesterol, sitosterol, pyrene, and naphthalene, respectively.[13] The fact that the sterols are more stable than aromatics for solubilization due to their resemblance to the solubilizer structure is also indicated. Therefore, the number of cross-peaks for sterol-solubilized solutions is less than that for aromatic-solubilized solutions. However, the direct solubilization site for sterols in micelle could not be intrinsically determined due to overlapped signal between sterols and bile salts as shown in Fig. 3. As shown in the ROESY spectrum of Fig. 4d, the weak cross-peaks for naphthalene and 19-methyl protons of NaTDC were directly observed in the downfield area. Similarly, the other aromatics of the pyrene solution had similar cross-peaks, as shown in Fig. 4e. Therefore, the solubilization of aromatics into micelles reveals some new pairs in addition to the pairs of the pure micellar solution, as shown in Table 2. The ROESY spectra for the aromatics solubilized in micellar solutions supported the result of the T_1 data (described in the next chapter); they were solubilized between micellar back-to-back sites.

***T*$_1$ Measurement.** The spin-lattice relaxation time (longitudinal relaxation time: T_1), which is based on the molecular dynamics of rotational motion, is a useful parameter for investigating the micellar structure. A pure NaTDC solution with a relaxation time of T_1 was used to establish a standard for the rotational motion of a proton in monomer (1 mM) and micellar (15 and 25 mM) solutions; this is shown in Table 3 and Fig. 5. They can be used for comparing the solubilized solutions of T_1 to the standard pure micellar solution, as elaborated in the next

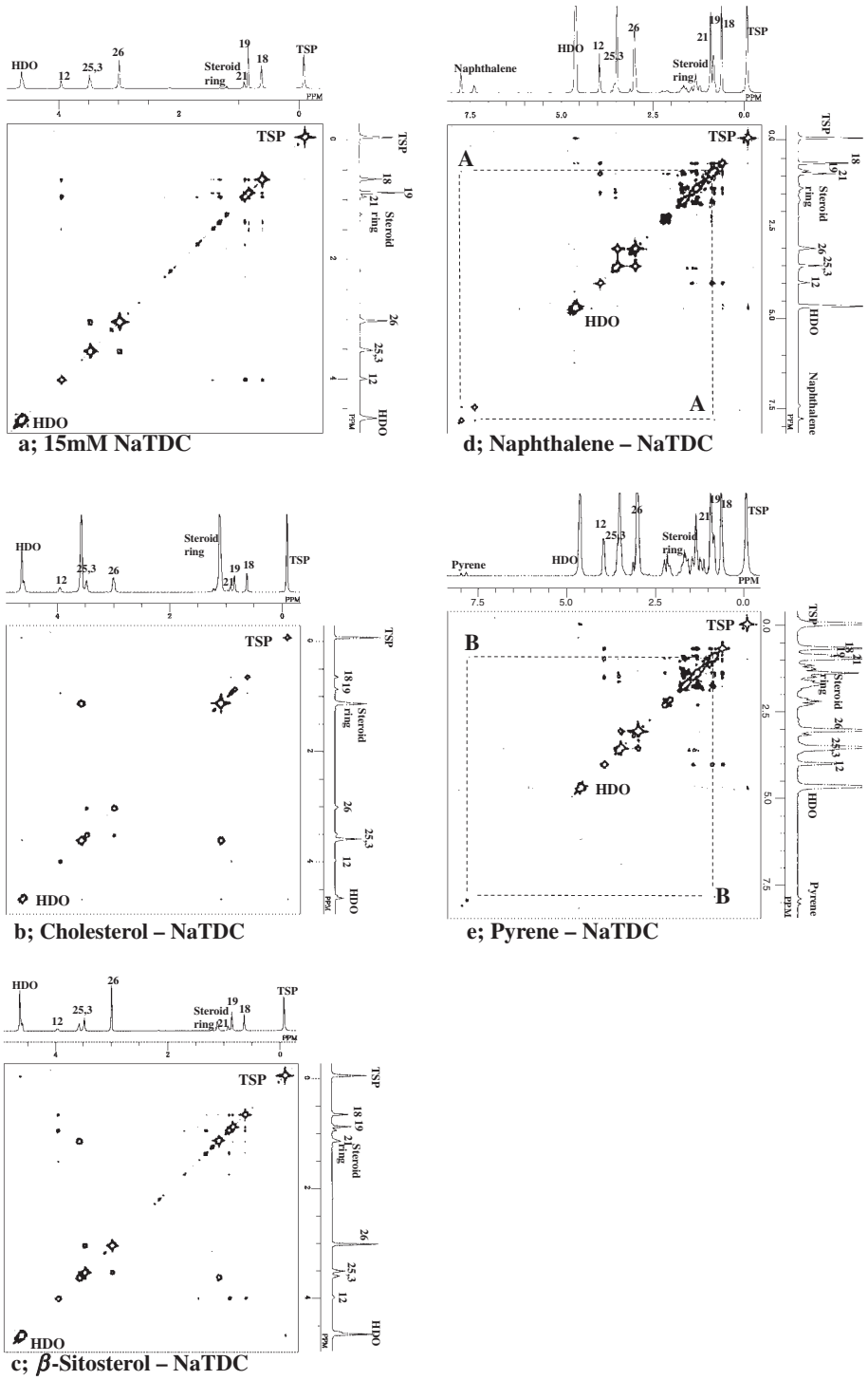

Fig. 4. Contour plots of the saturated solubilizates of NaTDC solutions (15 mM) from the ROESY measurements. The condition of each solution is as follows. a: pure micellar solution of NaTDC (15 mM); b: saturated cholesterol–NaTDC; c: saturated β-sitosterol–NaTDC; d: saturated naphthalene–NaTDC; and e: saturated pyrene–NaTDC. The concentrations of the solubilizates correspond with those shown in Fig. 2. A and B in Figs. 4d and 4e indicate cross-peaks between naphthalene and the 19-methyl group and pyrene and the 19-methyl group, respectively.

paragraph. As shown in Fig. 5, the T_1 value in the monomer state was considerably larger than that in the micellar state for all proton positions. This indicated that the degree of rotational motion of protons in the bile salt molecules decreased after micelle formation. A smaller value of T_1, i.e., rapid recovery time to stationary state, suggests that the rotational motion of protons is restricted due to the intramicellar and intermicellar interactions. The difference between T_1 for the monomer and micellar solutions is larger for a relatively hydrophilic site than that for the hydrophobic sites on the division of NaTDC molecules into two surfaces.

The technique of T_1 measurement during micellization can

Table 2. H Pair of NaTDC Molecules from Intra- and Intermicellar Interactions by ROESY Spectra (+)[a)]

	Pair of cross-correlation peak for satulated solubilizate of NaTDC solution				
Pair	Pure micelle	Cholesterol	β-Sitosterol	Naphthalene	Pyrene
3β–7α	−	+	+	−	−
5α–$18CH_3$	−	−	−	+	+
5α–$19CH_3$	−	−	−	+	−
5α–$21CH_3$	+	−	−	+	−
6α–17α	−	−	−	−	+
7α–16β	−	+	−	−	−
11α–$19CH_3$	−	−	−	+	−
11α–$18CH_3$	−	−	−	−	+
12β–$18CH_3$	+	−	−	+	+
12β–$21CH_3$	+	+	+	+	+
$18CH_3$–$19CH_3$	+	+	+	+	+
$18CH_3$–$21CH_3$	+	+	+	+	+
$19CH_3$–$21CH_3$	+	−	−	−	−
$19CH_3$–7.8 ppm	−	−	−	+	−
$19CH_3$–8.1 ppm	−	−	−	−	+

a) The concentrations of solubilizates correspond with those shown in Fig. 2.

Table 3. T_1 Values for Monomer, Micellar Solutions, and Saturated Solubilizates of NaTDC Solutions (15 mM) at 308.2 K[a)]

		Pure system of NaTDC			15 mM NaTDC + solubilizate			
H Position	Chemcal shift /ppm	1 mM /μs	15 mM /μs	25 mM /μs	Cholesterol /μs	β-Sitosterol /μs	Naphthalene /μs	Pyrene /μs
1α	1.78	—	275 ± 3	311 ± 2	262 ± 7	256 ± 11	272 ± 5	270 ± 3
1β	0.99	428 ± 27	357 ± 5	354 ± 5	349 ± 11	348 ± 7	350 ± 5	355 ± 10
3β	3.54	906 ± 24	694 ± 10	672 ± 15	670 ± 17	683 ± 18	692 ± 9	703 ± 16
12β	4.03	518 ± 21	430 ± 8	420 ± 9	412 ± 18	397 ± 11	432 ± 9	439 ± 11
18	0.71	454 ± 5	375 ± 6	374 ± 3	371 ± 8	369 ± 5	376 ± 2	386 ± 6
19	0.93	463 ± 14	366 ± 8	360 ± 4	360 ± 10	361 ± 4	368 ± 3	378 ± 5
21	1.00	385 ± 6	356 ± 2	362 ± 3	350 ± 7	346 ± 6	361 ± 6	366 ± 8
23β	2.23	437 ± 9	366 ± 11	375 ± 15	315 ± 16	302 ± 18	330 ± 15	321 ± 8
25α	3.57	908 ± 31	729 ± 10	705 ± 6	708 ± 14	720 ± 13	720 ± 10	732 ± 10
26α	3.08	1279 ± 30	839 ± 13	782 ± 9	826 ± 7	827 ± 16	827 ± 18	835 ± 10

a) The concentrations of solubilizates correspond with those shown in Fig. 2.

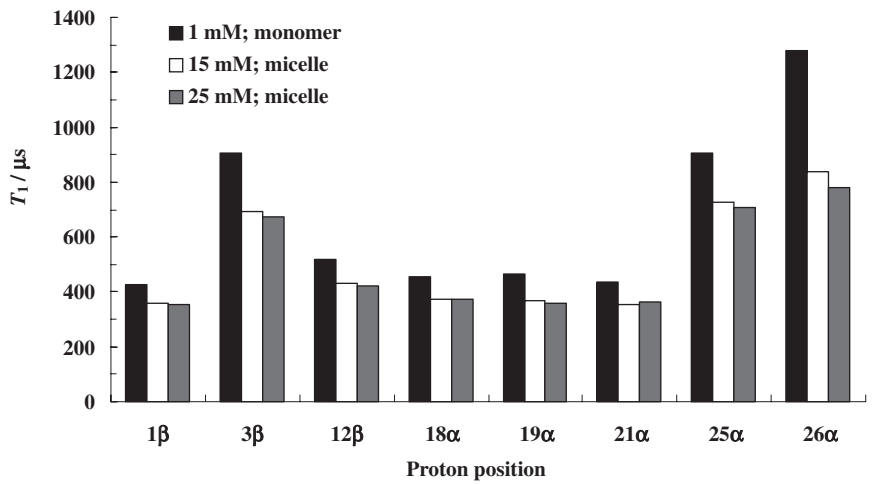

Fig. 5. Selected proton signals for T_1 in monomer (1 mM) and micellar (15 and 25 mM) solutions. All the proton numbers correspond to sodium taurodeoxycholate (Fig. 1).

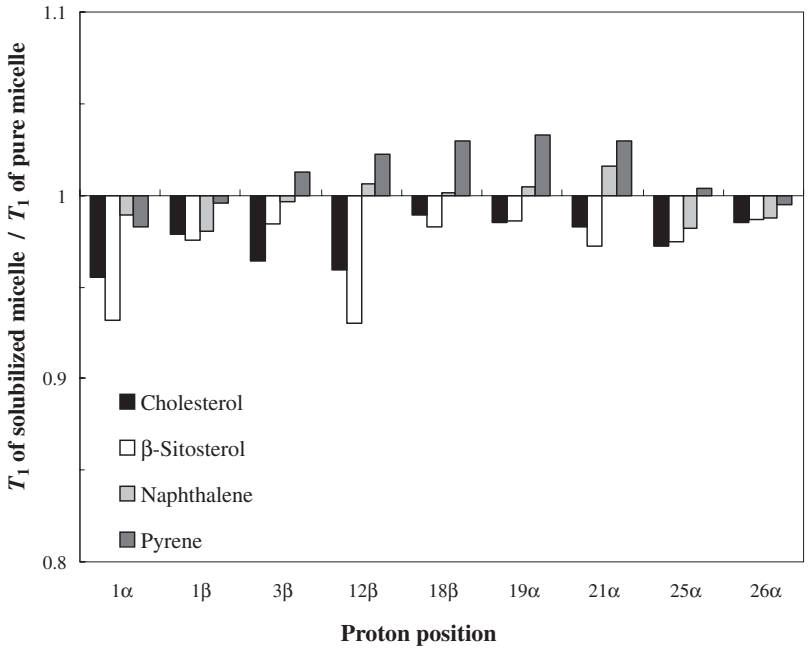

Fig. 6. T_1 ratio of the solubilized micelle to a pure micelle for a selected proton. All the proton numbers are equivalent to sodium taurodeoxycholate (Fig. 1). These ratios indicate the extent of the rotational motion of a proton in the micellar core.

be applied to solubilization systems comprising a saturated solubilizate such as the 15 mM NaTDC solution. The obtained T_1 values for a solubilized micellar solution at selected proton positions are shown in Table 3 and Fig. 6; the vertical axis represents the ratio of T_1 for the solubilized micellar solution to that for the pure micellar solution. Judging from the obtained T_1 ratios in Fig. 6, the solubilizates can be classified into two groups: sterols and aromatics. The T_1 values for solubilizates containing cholesterol or sitosterol are consistently low as compared to those for a pure micellar solution, which indicates that they could be solubilized to micellar cores via steroid interactions. Moreover, the degree of rotational motion of the bile salt molecules is restricted to a greater extent in the micellar core by the solubilizing sterols. From the viewpoint of the hydrodynamic radius of micelles, cholesterol-solubilized micelles formed a more compact packing of micelles as compared to pure micelles (12–15 Å as compared to 14–22 Å).[22] As long as there is a small difference in the T_1 values between solubilized and pure micelles, the intrinsic micellar properties for the solubilizing solution do not change considerably from those for the pure micellar solution. This is because they cannot solubilize the micellar solution in large amounts. According to our previous paper, the average number of cholesterol molecules per micelle was 0.44 in the 15 mM NaTDC of buffer solution on the basis of mass action model for the solubilization.[13,23] On the other hand, Figure 6 shows that the T_1 values of naphthalene- and pyrene-solubilized solutions are slightly increased at 12-, 18-, 19-, and 21-methyl positions. The increasing tendency of T_1 at a specific site is clearly different from its behavior in the sterol-solubilized solution, which may imply that the planar and bulky structures of aromatics penetrate the hydrophobic faces in the palisade layer. According to the Small model, the primary micelles of the bile salt are formed by hydrophobic back-to-back interactions.[24] Therefore,

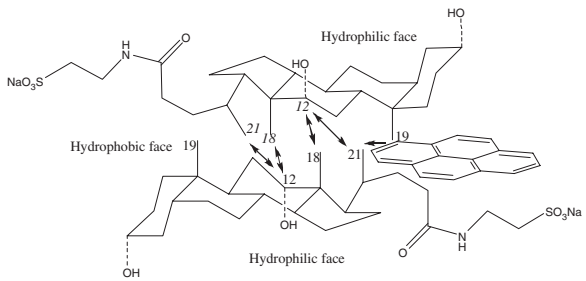

Fig. 7. Image of the estimated pyrene solubilization site in the micellar core. The bile salt containing methyl protons at 19 positions is directly influenced by the solubilized pyrene based on ROESY measurements.

the close packing of micelles is slightly loosened by aromatics penetrating the micelle. For example, the image of the estimated solubilization site of pyrene in the micelle is depicted in Fig. 7 on the basis of the T_1 and ROESY experiments. Therefore, the absence of competitive solubilization between cholesterol and pyrene, as shown in Fig. 2, is attributed to the difference in their solubilization sites.

Conclusion

Both ROESY and T_1 techniques are complementary, leading to the conclusion that cholesterol and β-sitosterol are solubilized to fit the micellar structure via the steroid–steroid interactions, and the obtained parameters are almost similar for cholesterol and β-sitosterol. The lowering of the cholesterol solubility in the presence of β-sitosterol is interpreted as β-sitosterol being preferentially solubilized at a similar solubilization site of the micelle according to the ΔG° values for the solubilization. On the other hand, pyrene and naphthalene are mainly solubilized in micellar palisade layer interacting with bile salt of methyl protons. Competitive solubilization between

the cholesterol and aromatics is not observed because their solubilization sites are rather different.

The authors are grateful to Showa Pharmaceutical University for funding this study, a collaboration with the Faculty of Pharmaceutical Sciences, Nagasaki International University.

References

1 E. A. Trautwein, G. S. M. J. E. Duchateau, Y. Lin, S. M. Mel'nikov, H. O. F. Molhuizen, F. Y. Ntanios, *Eur. J. Lipid Sci. Technol.* **2003**, *105*, 171.

2 M. Sugano, *Foods Food Ingredients J. Jpn.* **2005**, *210*, 490.

3 S. M. Mel'nikov, J. W. M. Seijen ten Hoorn, A. P. A. M. Eijkelenboom, *Chem. Phys. Lipids* **2004**, *127*, 121.

4 A. M. Lees, H. Y. Mok, R. S. Lees, M. A. McCluskey, S. M. Grundy, *Atherosclerosis* **1977**, *28*, 325.

5 A. de Jong, J. Plat, R. P. Mensink, *J. Nutr. Biochem.* **2003**, *14*, 362.

6 N. Funasaki, M. Fukuba, T. Hattori, S. Ishikawa, T. Okuno, S. Hirota, *Chem. Phys. Lipids* **2006**, *142*, 43.

7 M. Ueno, Y. Takamura, S. Nagadome, G. Sugihara, K. Takahashi, *Colloids Surf., B* **2000**, *19*, 43.

8 N. Funasaki, M. Fukuba, T. Kitagawa, M. Nomura, S. Ishikawa, S. Hirota, S. Neya, *J. Phys. Chem. B* **2004**, *108*, 438.

9 E. Kolehmainen, *Magn. Reson. Chem.* **1988**, *26*, 760.

10 B. M. Fung, L. Thomas, Jr., *Chem. Phys. Lipids* **1979**, *25*, 141.

11 C. Dominguez, C. Sebban-Kreuzer, O. Bornet, B. Kerfelec, C. Chapus, F. Guerlesquin, *FEBS Lett.* **2000**, *482*, 109.

12 S. Gouin, X. X. Zhu, *Langmuir* **1998**, *14*, 4025.

13 K. Matsuoka, T. Hirosawa, C. Honda, K. Endo, Y. Moroi, O. Shibata, *Chem. Phys. Lipids* **2007**, *148*, 51.

14 C. C. Allain, L. S. Poon, C. S. Chan, W. Richmond, P. C. Fu, *Clin. Chem.* **1974**, *20*, 470.

15 W. Richmond, *Clin. Chem.* **1973**, *19*, 1350.

16 H. Sugioka, Y. Moroi, *Biochim. Biophys. Acta* **1998**, *1394*, 99.

17 K. Matsuoka, M. Suzuki, C. Honda, K. Endo, Y. Moroi, *Chem. Phys. Lipids* **2006**, *139*, 1.

18 R. D. Stevens, A. A. Ribeiro, L. Lack, P. G. Killenberg, *J. Lipid Res.* **1992**, *33*, 21.

19 D. V. Waterhous, S. Barnes, D. D. Muccio, *J. Lipid Res.* **1985**, *26*, 1068.

20 J. P. M. Ellul, G. M. Murphy, H. G. Parkes, R. Z. Slapa, R. H. Dowling, *FEBS Lett.* **1992**, *300*, 30.

21 S. P. Sawan, T. L. James, L. D. Gruenke, J. C. Craig, *J. Magn. Reson.* **1979**, *35*, 409.

22 S. Nagadome, A. Yamauchi, K. Miyashita, H. Igimi, G. Sugihara, *Colloid Polym. Sci.* **1998**, *276*, 59.

23 K. Matsuoka, M. Maeda, Y. Moroi, *Colloids Surf., B* **2003**, *32*, 87.

24 D. M. Small, *Adv. Chem. Ser.* **1968**, *84*, 31.